

SCIENTIFIC REPORTS



OPEN

Moderate fabrication and characterization of the microcrystalline Sr_2CuO_3 glass films with effective nonlinearities

Tao Xu, Guangcai Hu, Jutao Jiang, Congfei Yin, Run Xiang, Xiaojuan Liang & Weidong Xiang

Since nonlinear optical materials used in the ultrafast all-optical switching is an important part for the modern optical technology, cuprates have been widely investigated for their specific Cu-O chain structure and intriguing optical properties. We present a new preparation method of microcrystalline Sr_2CuO_3 glass films on glass substrates combining spin-coating and co-sintering techniques. Then, the as-prepared samples were polished for different times to obtain microcrystalline Sr_2CuO_3 glass films with varying thickness. The influence of polishing time on the structure, the valence state and the nonlinear optical response were discussed, respectively. The purity of the Sr_2CuO_3 phase, surface morphology and the chemical composites of these synthesized glass films were given with scanning electron microscopy (SEM), energy dispersive X-ray spectroscopy (EDS), X-ray powder diffraction (XRD) and X-ray photoelectron spectroscopy (XPS). Importantly, optical absorption spectroscopy and Z-scan technique were used to measure linear absorption and third-order optical nonlinearity of the films. The experiments showed that third-order nonlinear susceptibility of the 140 min polished film sample with a thickness of $18 \mu\text{m}$ was up to 1.23×10^{-12} esu, indicating its potential application in the nonlinear field.

In recent decades, cuprates with one-dimensional electronic structure have been of particular importance in superconductivity and nonlinear optics due to the extreme CuO_2 structure and the motion of electrons in a confined space¹⁻³. Naturally, Sr_2CuO_3 , as a typical representative of one-dimensional Mott insulator of cuprates, have been widely investigated for its active role in the preparation of superconductors and unusual nonlinear response⁴⁻⁸. In more general terms, the structure of Sr_2CuO_3 is similar to that of the two-dimensional compound La_2CuO_4 , which only lacks oxygen atoms in Cu-O chains between the Cu ions in the *c*-axis direction, therefore, Sr_2CuO_3 is a favorable precursor for the synthesis of Cu-O composites⁹⁻¹². Previous studies focus much on searching for the analogs of Sr_2CuO_3 or introducing other metallic elements to enhance the superconductivity of the final product. For example, Koushik Karmakar prepared single crystal SrCuO_2 using the Traveling Solvent Floating Zone (TSFZ) Method and studied its magnetic property¹³. After that, Koushik Karmakar successfully achieved crystal growth of spin chain compound Sr_2CuO_3 doped with Zn, Co, Ni and Mn and analyzed quantum defect in a spin 1/2 chain¹⁴. Additionally, T. Geballe synthesized the $\text{Sr}_{2-x}\text{Ba}_x\text{CuO}_{3+\delta}$ through a traditional solid state method, mainly to enhance the superconductivity of the cuprates with the doping of Ba atoms¹⁵. The used Sr_2CuO_3 powder is mostly synthesized through the traditional solid state method, and the electronic structure and superconductivity of the related materials are investigated¹⁶⁻²⁰. However, these studies had been devoted to understand the structure and size of Sr_2CuO_3 particles, lacking the exploration in nonlinear applications field. Fortunately, the Sr_2CuO_3 with large third-order nonlinearity had also been reported in 2000. H. Kishida studied the third-order nonlinearity of one-dimensional Mott insulators of Sr_2CuO_3 thin film and analyzed the nonlinear enhancement mechanism for the first time²¹. Additionally, T. Ogasawara reported high third-order susceptibility $\chi^{(3)}$ at optical fiber communication and room temperature ultrafast recovery on Sr_2CuO_3 thin film, indicating the strong potential of Sr_2CuO_3 to fabrication of all-optical switching devices²². Besides that, H. Kishida obtained third-harmonic generation spectra in single-crystalline thin films of Sr_2CuO_3 and Ca_2CuO_3 ²³. The two-photon resonant structure demonstrates that the even-charge transfer states are located close to the

College of Chemistry and Materials Engineering, Wenzhou University, Wenzhou, 325035, China. Correspondence and requests for materials should be addressed to X.L. (email: lxj6126@126.com) or W.X. (email: xiangweidong001@126.com)

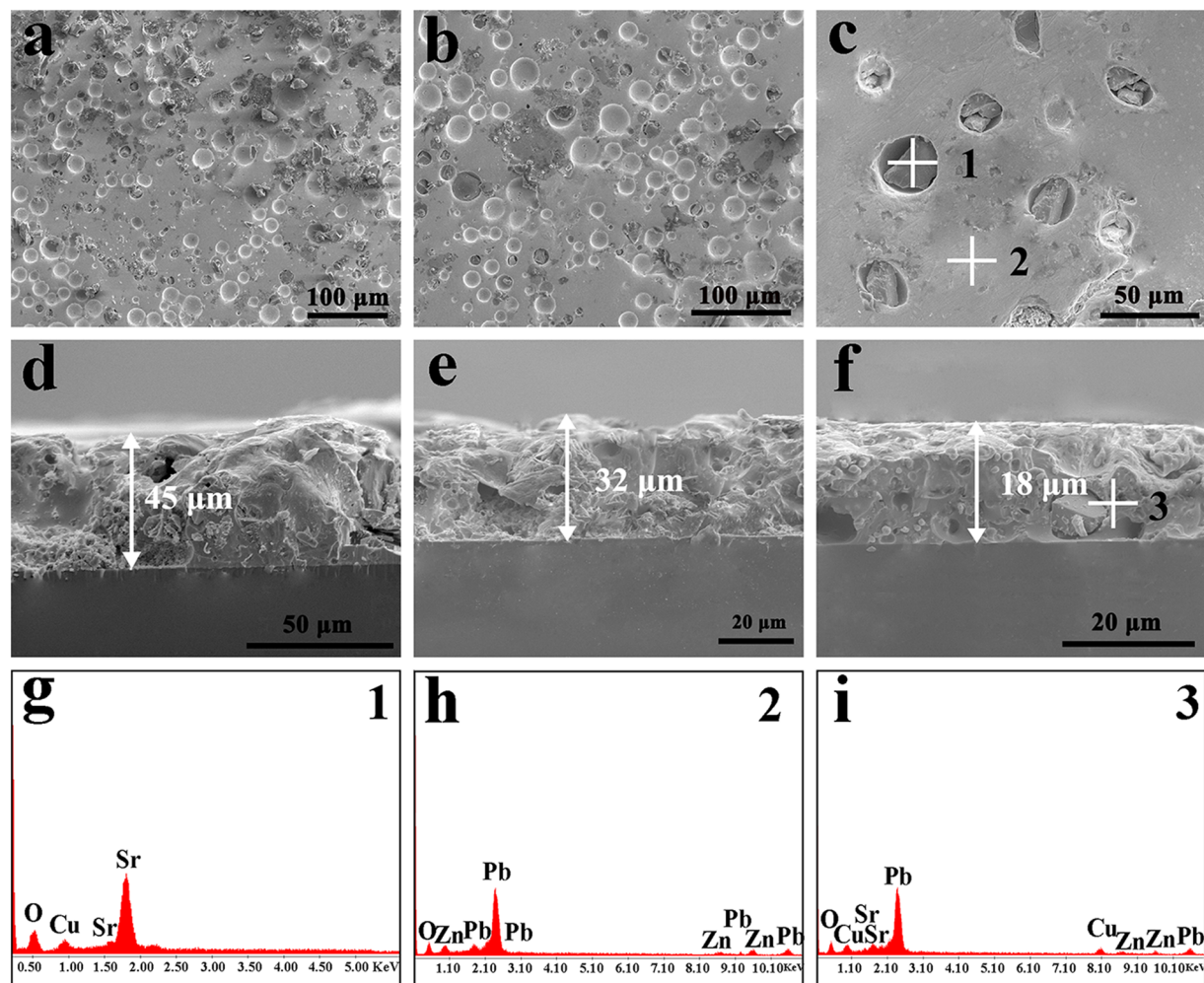


Figure 1. Morphology and structural characterization of the microcrystalline Sr_2CuO_3 glass films polished different times under 500°C sintering: (a)/(d) 60 min, (b)/(e) 100 min and (c)/(f) 140 min. The EDS images of the microcrystalline Sr_2CuO_3 glass film polished for 140 min at three points (g) 1, (h) 2 and (i) 3.

odd-charge transfer states. After that, M. Ohtani revealed the synthesis of desired orientations and high crystallinity for $(\text{Sr}_x\text{Ca}_{1-x})_2\text{CuO}_3$ thin films and the linear relation of x and the charge transfer gap²⁴. Furthermore, A. Maeda had successfully grown Sr_2CuO_3 crystals on the LaAlO_3 substrate, and then discussed its nonlinear property with Ca_2CuO_3 to considering excitonic effect²⁵. In a word, scholars prepare Sr_2CuO_3 materials with the use of pulsed laser deposition (PLD), TFSZ and RF magnetron sputtering techniques, which are always labor-intensive and time-consuming with the instrument hard to manipulate. Furthermore, the research of the thickness dependence of structure and optical property for the microcrystalline Sr_2CuO_3 films is seldom reported.

In this paper, microcrystalline Sr_2CuO_3 glass films were obtained by combining co-sintering and spin-coating technique for the first time^{26,27}. The Sr_2CuO_3 particles were firmly embedded in the Pb-glass matrix on the surface of K_9 glass substrate. Subsequently, through mechanical polishing for different times, different thicknesses of film samples were acquired. Thickness dependence of structure and optical property for the microcrystalline Sr_2CuO_3 glass films were investigated in detail. As a result, the final Z-scan experiment showed that the 140 min polished microcrystalline Sr_2CuO_3 glass film with a thickness of $18\ \mu\text{m}$ owned a fast nonlinear response, could be a suitable nonlinear optical candidate compared to some known materials²⁸.

Results and Discussion

SEM and EDS analysis. To capture the transformation of the morphology and elements distribution in the microcrystalline Sr_2CuO_3 glass film under the polishing process, SEM and EDS spectra analyses were conducted. Figure 1a–c provide the SEM images of the microcrystalline Sr_2CuO_3 glass film at three polishing times: 60, 100 and 140 min under 500°C sintering, as an example. The as-prepared films reveal that the gray microcrystalline Sr_2CuO_3 particles were tightly embedded in the Pb-glass layer, which were fabricated by using co-sintering the original materials, and they were adhered to the surfaces in the K_9 glass substrates. With the increase of polishing times, the surfaces of microcrystalline glass film transformed from rough and holey morphology to relatively well-distributed and smooth surfaces. As though there are still some sporadic holes exist in the cross-sections of the various film sample, and the smooth skin layers illustrate the polishing process could effectively adjust the

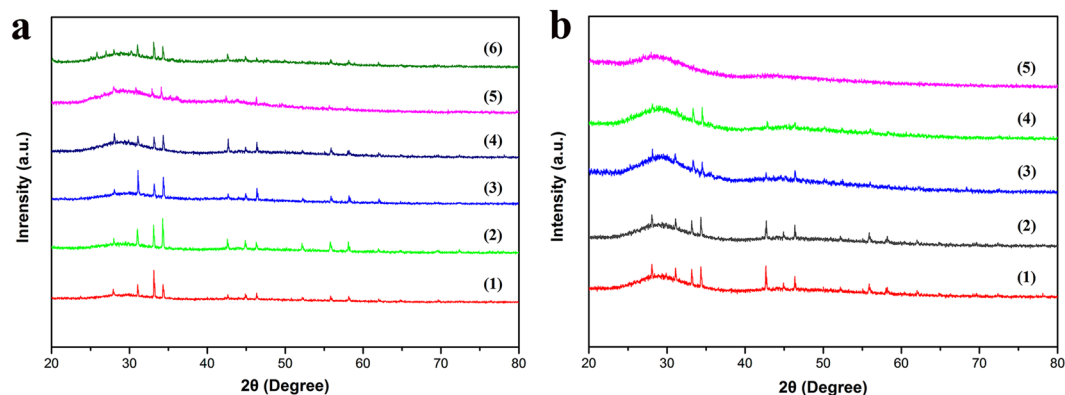


Figure 2. (a) Comparison of powder XRD patterns of the microcrystalline Sr_2CuO_3 glass films with different sintering temperatures (1) 100 °C, (2) 200 °C, (3) 300 °C, (4) 400 °C, (5) 500 °C and (6) 600 °C. (b) Comparison of powder XRD patterns of the microcrystalline Sr_2CuO_3 glass films polished different times under 500 °C sintering (1) 0 min, (2) 60 min, (3) 100 min, (4) 140 min and (5) 180 min.

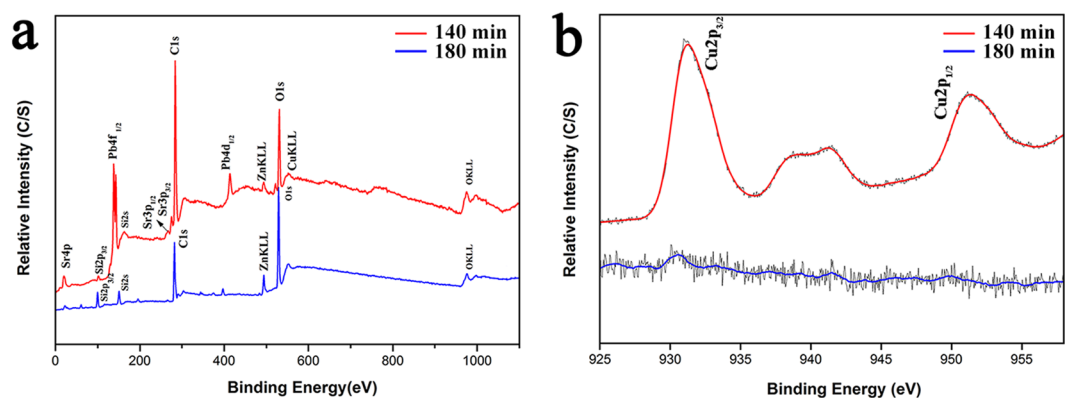


Figure 3. XPS spectra of the film samples polished 140 min and 180 min under 500 °C sintering: (a) full XPS spectra and (b) the high-resolution spectra for $\text{Cu}2p$.

film thickness, as shown in Fig. 1d–f. Additionally, by measurement, the corresponding thicknesses of these film samples polished for 60 min, 100 min, 140 min were 45, 32 and 18 μm , respectively. The unique structure and steerable thickness of the as-synthesized film samples have a large impact on the valence state and the nonlinear optical response, which will be discussed below. Furthermore, the EDS spectra of these film samples are presented in Fig. 1g–i, revealing there are no impurities in these films except the Sr_2CuO_3 particles and the Pb-glass matrix.

XRD analysis. To assess the influence of the dependence of synthesis temperature and polishing time on the structure of microcrystalline Sr_2CuO_3 glass film, the XRD patterns are presented in Fig. 2. The crystalline and purity of microcrystalline Sr_2CuO_3 glass film sintered at 100 °C to 600 °C orderly may be depicted as in Fig. 2a. Obviously, the diffraction patterns correspond to the JCPDS 85–2487 (Sr_2CuO_3) from 100 °C to 500 °C. No extra peaks are detected, which indicate that the Sr_2CuO_3 has a single-phase structure during the whole heating process. Nevertheless, there are some extra peaks conforming to PbO and SrPbO_3 appear when the sinter temperature rise up to 600 °C, mainly attribute to the interaction between Sr_2CuO_3 and the glass compositions. In addition, Fig. 2b shows the effect of different polishing times vary from 0 to 180 min on the particle size of microcrystalline film prepared at 500 °C, considering the better combination of glass substrate and Sr_2CuO_3 particles and phase purity. We can see that as the polishing time increases, the intensity of the diffraction peak gradually decreases. From the XRD patterns of the microcrystalline Sr_2CuO_3 glass film polished for 180 min, we could assume that the surface of the film sample is K_9 glass substrate. Similarly, all the XRD patterns exhibit a large amorphous peak with 2θ at approximately $28^\circ\sim 32^\circ$ attributing to the diffraction from the glass matrix.

XPS analysis. With the purpose of evaluating the effect of the thermal treatment and polish procedure on the valence state and element type of the microcrystalline Sr_2CuO_3 glass films, ulteriorly, the XPS was performed to analyze the as-prepared samples polished for 140 min and 180 min under sintering temperature of 500 °C. Figure 3a depicts the survey XPS spectra of these two glass films correspond to the red and blue curves for the samples polished for 140 min and 180 min, respectively. From the red curve, we can observe that the peaks of Pb, Zn, Si, Sr, Cu and O were presented in the as-synthesized glass film, agreeing with glass composition and Sr_2CuO_3 .

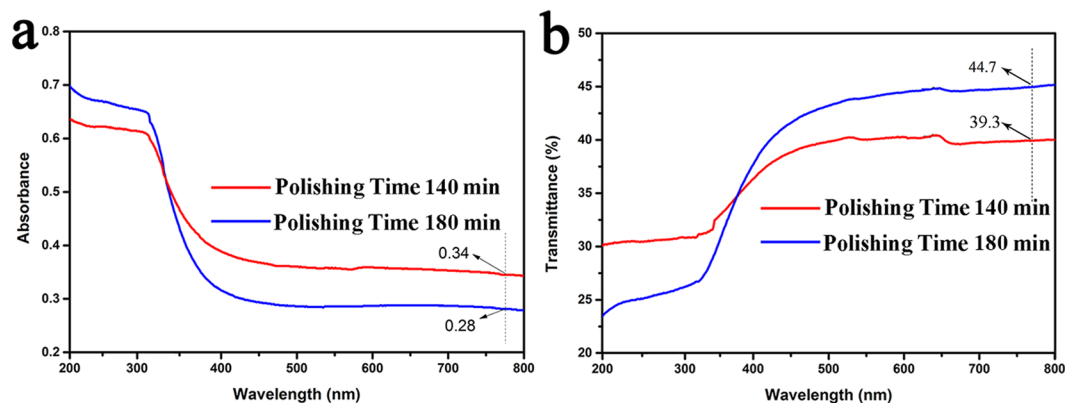


Figure 4. UV/VIS spectra of the film samples polished 140 min and 180 min: (a) Linear optical absorption spectra and (b) transmittance spectra.

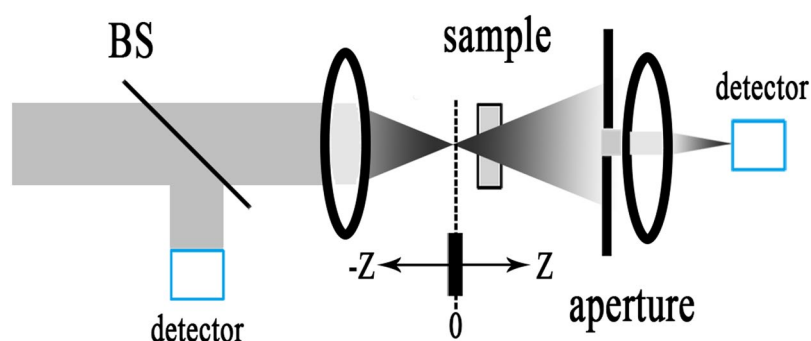


Figure 5. Schematic diagram of the OA (a) and CA (b) Z-scan experiment.

From XPS and fitting curves, we can calculate that the atomic ratio of Sr and Cu was 2:1, which correspond to the theoretical value (Sr_2CuO_3 particles). Meanwhile, the film sample polished for 180 min was also tested, mainly contain Zn, Si, and O from the blue curve, indicating that the film sample was in accordance with the K_9 glass substrate under excessive polishing procedure and no external element was introduced. Additionally, the high-resolution spectra for Cu 2p in these two film samples polished for 140 min and 180 min were showed in Fig. 3b. The red curve gives two peaks of Cu $2p_{3/2}$ and Cu $2p_{1/2}$ at approximately 931.9 eV and 951.16 eV, respectively, illustrating the valence state of Cu in the film sample is +2 or +1²⁸. As for the other, the Cu signals don't appear on the blue curve. Obviously, the red curve in Fig. 3b shows a precisely characteristic peak of Cu^{2+} at about 942.16 eV between the two strong peaks conforming to the XRD analysis of the 140 min polished microcrystalline Sr_2CuO_3 glass film.

Third-order optical nonlinearity. Optical absorption spectroscopy and Z-scan technique were used to measure linear absorption and third-order optical nonlinearity of the microcrystalline Sr_2CuO_3 glass films. Linear optical absorption of the film samples polished for 140 min and 180 min are described in Fig. 4a. In general, while for the sample with a lower transmittance (less than 30%), most of the testing energy are absorbed by the sample in the process, causing an increase of thermal effects on the sample. The linear optical absorption includes the linear loss. Figure 4b reveals that the transmittance of the glass film is about 40% at a wavelength of 787 nm, meeting the essential requirements of the Z-scan measurements. While the other glass films polished for shorter time would gather high powers on the surface under excitation laser irradiation, affecting the accuracy of measurement seriously for the lower transmittance.

The Z-scan is a single excitation beam technique to measure the nonlinear refractive index and nonlinear absorption coefficient of the materials²⁹. As can be easily understood, Fig. 5 simply shows schematic diagram of the Open-aperture (OA) and closed-aperture (CA) Z-scan experiment. The nonlinear refraction and absorption of the microcrystalline Sr_2CuO_3 glass films polished for 140 and 180 min were acquired by using OA and CA Z-scan technology. As shown in Fig. 6, the hollow triangles represent the measure results and the solid line show the theoretical fit of the normalized transmittance. Figure 6a and b give the OA and CA Z-scan results for the microcrystalline Sr_2CuO_3 glass film polished for 140 min. The film sample polished for 180 min was contrasted for reference shown in Fig. 6c,d. We can see that this is the reverse saturable absorption in the microcrystalline Sr_2CuO_3 glass film on account of the single symmetrical valley of peak relative to the focus ($z=0$) of the solid line in Fig. 6a. Meanwhile, Fig. 6b displays the signature of valley of peak indicating the occurrence of self-focusing process and negative value for the nonlinear refractive index ($\gamma < 0$) in the film sample at CA measurements. As

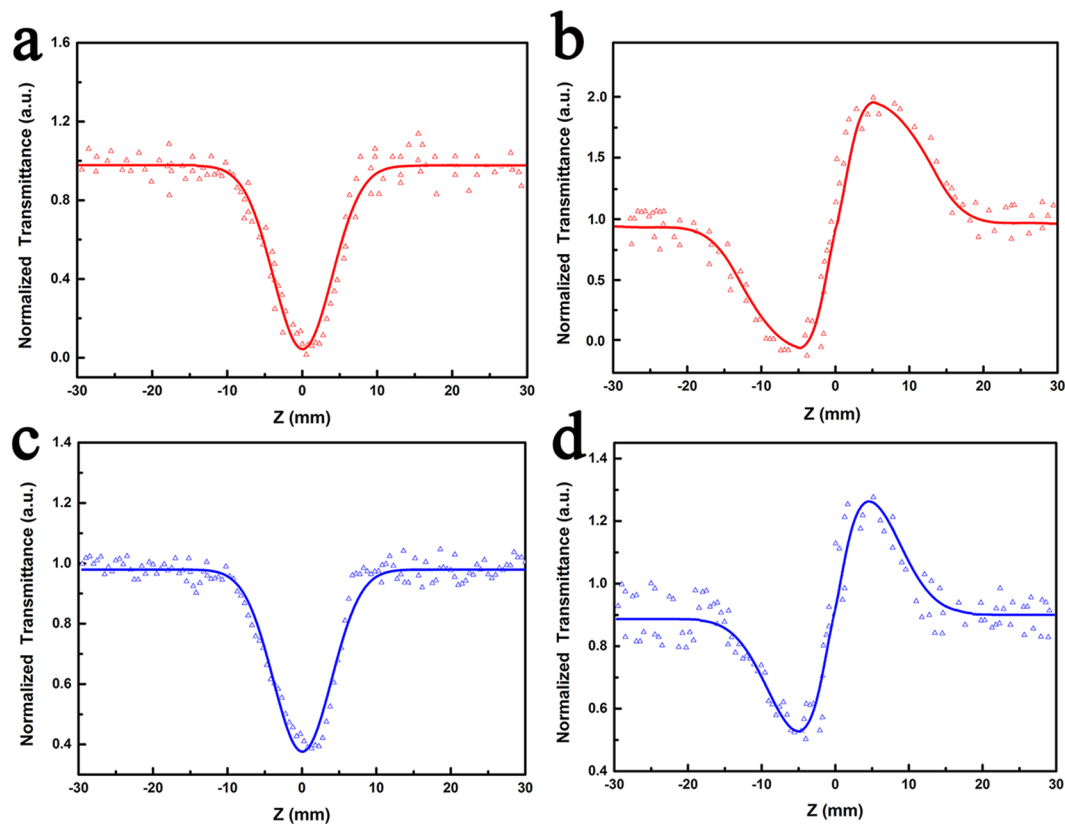


Figure 6. OA signal (a) and CA signal (b) of the film sample polished for 140 min. OA signal (c) and CA signal (d) of the film sample polished for 180 min.

well for the glass substrate in Fig. 6c,d, the signature is similar to the film sample polished for 140 min but the intensity is relatively weak.

According to a well-known theory³⁰, from the OA and CA Z-scan curves, we can calculate the nonlinear absorption coefficient (β) and nonlinear refractive index (γ) of the film. Furthermore, we can calculate the real and imaginary parts of the third-order nonlinear susceptibility ($\chi^{(3)}$) of the film samples by equations (1) and (2)³¹,

$$\text{Im}\chi^{(3)}(\text{esu}) = \frac{\lambda \varepsilon_0 c^2 n_0^2}{4\pi^2} \beta (\text{m/W}) \quad (1)$$

$$\text{Re}\chi^{(3)}(\text{esu}) = \frac{\varepsilon_0 c^2 n_0^2}{\pi} \gamma (\text{m}^2/\text{W}) \quad (2)$$

where n_0 , c , ε_0 and λ are linear refractive index, speed of light, permittivity of free space and the wavelength of the laser light of the film sample, respectively. The total third-order nonlinear susceptibility $\chi^{(3)}$ can be calculated by equation (3).

$$|\chi^{(3)}|(\text{esu}) = \{(\text{Re}\chi^{(3)})^2 + (\text{Im}\chi^{(3)})^2\}^{1/2} \quad (3)$$

As shown in Table 1, the parameters of third-order optical nonlinearity are listed. We introduced microcrystalline Sr_2CuO_3 in the Pb-glass matrix on the surface of K_9 glass substrate, and the results were expected to lead to a large third-order nonlinearity of the film sample, whose nonlinear susceptibility could be as high as 1.23×10^{-12} esu. Furthermore, we introduce the photon theory to explain the third-order nonlinear phenomenon more deeply. In the one-dimensional Cu-O composites, due to the occupied p-band of oxygen between the upper and lower Hubbard bands of the metal and the big field Coulomb interactions at the metal sites, the Mott-Hubbard gap opens in the d-band of copper²¹. The charge transfer between Cu and O is major determinant of the nonlinear optical response, while the Sr only serves as a bridge which concatenates the parallel Cu-O chains. In short, the absorption of photons and the dipole moment in the Cu-O composites result in the noticeably increase of third-order nonlinear susceptibility $\chi^{(3)}$ principally.

Conclusions

In a word, we report the synthesis of microcrystalline Sr_2CuO_3 glass films, which were fabricated by co-sintering and spin-coating technique. Next, through continuous polishing, we acquire microcrystalline films with various

Parameters	β (m/w)	$\text{Im}\chi^{(3)}$ (esu)	γ (m ² /w)	$\text{Re}\chi^{(3)}$ (esu)	$\chi^{(3)}$ (esu)
Microcrystalline Sr ₂ CuO ₃ film (140 min)	1.4×10^{-11}	4.69×10^{-13}	2.1×10^{-18}	1.14×10^{-12}	1.23×10^{-12}
Microcrystalline Sr ₂ CuO ₃ film (180 min)	3.7×10^{-13}	1.35×10^{-14}	8.9×10^{-20}	4.82×10^{-14}	5.0×10^{-14}

Table 1. Third-Order Nonlinear Optical Parameters of the film samples polished for 140 min and 180 min.

thicknesses. The changes of microcrystalline Sr₂CuO₃ glass films during the polishing process were monitored and discussed individually. From the analysis results of the SEM and EDS spectra, the Sr₂CuO₃ crystalline phase were well-embedded in the glass matrix. Additionally, the XRD patterns of the polished film samples exactly verified that the existence of Sr₂CuO₃ microcrystals in the glass matrices. At the same time, the composition and binding energy of Sr, Cu, and O were determined using the results of XPS curves. From XPS and calculations, we can concluded that the atomic ratio of Sr and Cu was 2:1, which correspond to the theoretical value (Sr₂CuO₃ particles). Benefiting from the results, third-order optical nonlinearities of the microcrystalline Sr₂CuO₃ glass films were measured through the Z-scan technique. The Z-scan experiment indicated that the microcrystalline Sr₂CuO₃ glass film has a terrific third-order optical nonlinearity with the $\chi^{(3)}$ as high as 1.23×10^{-12} esu, exhibiting its potential application in the nonlinear field.

Methods

Samples preparation. The Sr₂CuO₃ powder was prepared to use a traditional solid state method. SrO (99.99%) and CuO (99.99%) in stoichiometric amount were mixed evenly for 60 min, and the mixture was sintered at 980 °C for 20 h in the crucibles under an ambient atmosphere. After a short time, the subsequent acquired intermediates were again further heated at 980 °C for 10 h, with fully grindings. Subsequently, the Sr₂CuO₃ powder in grayish was obtained. It is pointed out that the synthesized Sr₂CuO₃ powder is hygroscopic, which should be stored in the dryer to avoid contact with moist air and carbon dioxide. After that, according to the ratio of 1:3 (mass fraction), the Sr₂CuO₃ and Pb-glass powder (PbO₂-ZnO-B₂O₃-SiO₂) were mixed homogeneously for 2 h. Then, their mixtures were blended with the naphtha evenly. The viscous composite was individually disposed on the surfaces of K₉ glass substrate through spin-coating technology with the rate of 2000 rpm for 30 s. Subsequently, we put the composites of Sr₂CuO₃ and glass powder on the K₉ glass substrates into the muffle furnace, and adjust the sintering temperature from 100 °C to 600 °C. Last, we acquired film samples, which were named microcrystalline Sr₂CuO₃ glass films by us, and the as-prepared samples were polished for different times to obtain microcrystalline Sr₂CuO₃ glass films with varying thickness.

Samples tests. All of the film samples, no matter what they prepared in any conditions, were subjected to structural and phase characterization with the X-ray diffraction (XRD, D8 Focus, Bruker, Germany) in the range of 20–80° (2 θ). In addition, the morphology and elements distribution in the microcrystalline Sr₂CuO₃ glass film were analyzed by field-emission scanning electron microscope (FE-SEM, Auriga, Carl Zeiss) with the measuring equipment of energy dispersive X-ray spectroscopy. The chemical compositions and the valence state of ions in the thin film surface were characterized with the X-ray photoelectron spectroscopy (XPS, SHI-MADZU) Furthermore, by using the UV/VIS Spectrophotometer (Mode V-570, JASCO), the linear absorption and transmittance spectra were acquired. Measurements of the third-order optical nonlinearities of the microcrystalline Sr₂CuO₃ glass film were determined by Z-scan method at 787 nm, and the pulse width, single-pulse energy and repetition rate were 397 fs, 0.1 μ J and 1000 Hz, respectively. All of the above tests of the film samples were conducted at room temperature.

Data availability. The datasets generated during the current study are available from the corresponding author on reasonable request.

References

- Sauteret, C. *et al.* Optical Nonlinearities in One-Dimensional-Conjugated Polymer Crystals. *Phys. Rev. Lett.* **36**, 956–959 (1976).
- Ghosh, H. & Chari, R. Gigantic stimulated Raman scattering in one-dimensional Mott–Hubbard insulators: A possible THz source. *Phys. Lett. A* **374**, 2379–2382 (2010).
- Ashida, M. *et al.* One-dimensional cuprate as a nonlinear optical material for ultrafast all-optical switching. *Appl. Phys. Lett.* **78**, 2831–2833 (2001).
- Bonvalot, M., Beaunon, E., Bourgault, D., Núñez-Ez-Regueiro, M. & Tournier, R. Ambient pressure synthesis of tetragonal Sr₂CuO_{3+x}. *Phys. C. Super.* **282**, 539–540 (1997).
- Takayama-Muromachi, E. & Matsui, Y. 1a-YK-4 High-pressure synthesis of new oxyphosphate superconductors II. *Chem. Mater.* **10**, 2686–2698 (1998).
- Mizuno, Y., Tsutsui, K., Tohyama, T. & Maekawa, S. Nonlinear optical response and spin-charge separation in one-dimensional Mott insulators. *Phys. Rev. B* **62**, R4769–R4773 (2000).
- Sota, S. & Tohyama, T. Density matrix renormalization group study of optical conductivity in the one-dimensional Mott insulator Sr₂CuO₃. *Phys. Rev. B* **82**, 6663–6674 (2010).
- Manako, T. *et al.* Orientation-controlled epitaxy of A₂CuO₃ (A: Sr, Ca) films with large optical nonlinearity. *Appl. Phys. Lett.* **79**, 1754–1756 (2001).
- Ami, T. *et al.* Magnetic susceptibility and low-temperature structure of the linear chain cuprate Sr₂CuO₃. *Phys. Rev. B* **51**, 5994–6001 (1995).
- Archibald, W. B., Zhou, J. S. & Goodenough, J. B. Transport properties of Cu-O chains in Sr₂CuO_{3+x}. *Phys. Rev. B* **52**, 16101 (1995).
- Ogasawara, T. *et al.* Ultrafast optical nonlinearity in the quasi-one-dimensional mott insulator Sr₂CuO₃. *Phys. Rev. Lett.* **85**, 2204 (2000).

12. Takahashi, K., Okai, B., Kosuge, M. & Ohta, M. Crystallographic Study in the $\text{Nd}_2\text{CuO}_4\text{-Sr}_2\text{CuO}_3$ System. *Jpn. J. Appl. Phys* **27**, L1374–L1376 (1988).
13. Karmakar, K., Singh, A., Singh, S., Poole, A. & Rüegg, C. Crystal Growth of the Nonmagnetic Zn^{2+} and Magnetic Co^{2+} Doped Quasi-One-Dimensional Spin Chain Compound SrCuO_2 Using the Traveling Solvent Floating Zone Method. *Cryst. Growth. Des.* **14**, 1184–1192 (2015).
14. Karmakar, K., Bag, R. & Singh, S. Crystal Growth of Spin Chain Compound Sr_2CuO_3 Doped with Quantum Defects: Zn, Co, Ni, and Mn. *Cryst. Growth. Des.* **15**, 4843–4853 (2015).
15. Gao, W. B. *et al.* Out of plane effect on the superconductivity of $\text{Sr}_{2-x}\text{Ba}_x\text{CuO}_{3+y}$ with Tc up to 98K. *Phys. Rev. B* **80**, 129–135 (2009).
16. Zhigadlo, N. D. *et al.* High-pressure synthesis and characterization of a new series of V-based superconductors $(\text{Cu}_{0.5}\text{V}_{0.5})\text{Sr}_2\text{Ca}_{n-1}\text{Cu}_n\text{O}_y$. *Chem. Mater.* **11**, 2185–2190 (1999).
17. Cao, Y., Qin, H., Niu, X. & Jia, D. Simple solid-state chemical synthesis and gas-sensing properties of spinel ferrite materials with different morphologies. *Ceram. Int.* **42**, 10697–10703 (2016).
18. Long-González, D. *et al.* Synthesis of monoclinic Celsian from Coal Fly Ash by using a one-step solid-state reaction process. *Ceram. Int.* **36**, 661–672 (2010).
19. Kurmaev, E. Z. *et al.* X-ray emission and photoelectron spectra, and the location of fluorine atoms in strontium and calcium copper oxyfluorides. *J. Phys. Condens. Mat.* **8**, 4847 (1996).
20. Dogruer, M., Gorur, O., Karaboga, F., Yildirim, G. & Terzioglu, C. Zr diffusion coefficient and activation energy calculations based on EDXRF measurement and evaluation of mechanical characteristics of $\text{YBa}_2\text{Cu}_3\text{O}_{7-x}$ bulk superconducting ceramics diffused with Zr nanoparticles. *Powder. Technol.* **246**, 553–560 (2013).
21. Kishida, H. *et al.* Gigantic optical nonlinearity in one-dimensional Mott-Hubbard insulators. *Nature* **405**, 929–932 (2010).
22. Ogasawara, T. *et al.* Ultrafast optical nonlinearity in the quasi-one-dimensional Mott insulator Sr_2CuO_3 . *Phys.Rev.Lett.* **85**, 2204 (2000).
23. Kishida, H. *et al.* Large third-order optical nonlinearity of Cu-O chains investigated by third-harmonic generation spectroscopy. *Phys. Rev. Lett.* **87**, 177401 (2001).
24. Ohtani, M., Fukumura, T., Sakurada, H., Nishimura, J. & Kawasaki, M. Synthesis and characterization of composition-spread $(\text{Sr,Ca})_2\text{CuO}_3$ thin films with high third-order optical nonlinearity. *Appl. Phys. Lett.* **83**, 842–844 (2003).
25. Maeda, A. *et al.* Third-order nonlinear susceptibility spectra of CuO chain compounds investigated by the Z-scan method. *Phys. Rev. B* **70**, 2516–2528 (2004).
26. Sonker, R. K., Sabhajeet, S. R. & Yadav, B. C. $\text{TiO}_2\text{-PANI}$ nanocomposite thin film prepared by spin coating technique working as room temperature CO_2 gas sensing. *J Mater. Sci: Mater. El.* **27**, 11726–11732 (2016).
27. Yang, H. *et al.* studies of $\text{Sr}_2\text{CuO}_{3+\delta}$ (nominal $\delta = 0.1\text{--}0.4$): Effect of apical oxygen ordering on TC of cuprate superconductors. *Physica. C* **467**, 59–66 (2007).
28. Ma, L. *et al.* Facile synthesis of tunable fluorescent carbon dots and their third-order nonlinear optical properties. *Dyes Pigments* **128**, 1–7 (2016).
29. Yin, C. *et al.* Facile synthesis of a glass film containing Ca_2CuO_3 micro-crystals and exhibiting a third-order non-linear property. *Ceram. Int.* **42**, 15897–15903 (2016).
30. Sheik-Bahae, M., Said, A. A., Wei, T. H., Hagan, D. J. & Stryland, E. W. V. Sensitive measurement of optical nonlinearities using a single beam. *IEEE J. of Quantum Elect.* **26**, 760–769 (2002).
31. Fan, G. *et al.* Mechanisms for fabrications and nonlinear optical properties of Pd and Pt nanoparticles by femtosecond laser. *Opt. Commun.* **295**, 219–225 (2013).

Acknowledgements

T.X. wishes to thank G.H., J.J., C.Y., R.X., X.L. and W.X. for fruitful discussions. This study was supported by the National Nature Science Foundation of China (51672192 and 51472183).

Author Contributions

T.X., G.H. and C.Y. conceived the study. T.X. G.H. and J.J. prepared the Sr_2CuO_3 glass film. T.X., G.H. and R.X. conducted the samples tests. T.X. and G.H. wrote the paper. All authors discussed the results and commented the manuscript.

Additional Information

Competing Interests: The authors declare no competing interests.

Publisher's note: Springer Nature remains neutral with regard to jurisdictional claims in published maps and institutional affiliations.



Open Access This article is licensed under a Creative Commons Attribution 4.0 International License, which permits use, sharing, adaptation, distribution and reproduction in any medium or format, as long as you give appropriate credit to the original author(s) and the source, provide a link to the Creative Commons license, and indicate if changes were made. The images or other third party material in this article are included in the article's Creative Commons license, unless indicated otherwise in a credit line to the material. If material is not included in the article's Creative Commons license and your intended use is not permitted by statutory regulation or exceeds the permitted use, you will need to obtain permission directly from the copyright holder. To view a copy of this license, visit <http://creativecommons.org/licenses/by/4.0/>.

© The Author(s) 2018